

An ESPRIT-Based Moving Target Sensing Method for MIMO-OFDM ISAC Systems

Yang Xiang^{ID}, Yuxing Gao^{ID}, Xinru Yang, Shanqing Kang, and Meiyun Shao^{ID}

Abstract—Integrated sensing and communications (ISAC) has recently attracted lots of research interest, in which using the MIMO-OFDM system to sense the moving targets is an important task. However, the existing FFT-based moving target sensing methods are severely limited by grid resolution, and the sensing scheme based on a single base station (BS) can only obtain the radial velocity of the target. To alleviate these issues, this letter transforms the problem of moving target sensing into a generalized array signal form, and then a moving target estimation method based on ESPRIT algorithm is proposed, realizing super-resolution and low-complexity estimation of target parameters. Moreover, we propose an actual velocity estimation scheme based on double BSs, in which the two-dimensional actual velocity vector can be estimated based on the radial velocities and the geometric relationship. Simulation results are provided to demonstrate the effectiveness of the proposed schemes.

Index Terms—Integrated sensing and communications, actual velocity estimation, MIMO-OFDM systems, ESPRIT.

I. INTRODUCTION

THE sixth generation (6G) mobile communications system is believed to be able to simultaneously realize ultra-high data rate communications and high-precision sensing, which has sparked widespread research interest in integrated sensing and communications (ISAC) systems [1], [2], [3], [4]. Among the diverse tasks that the ISAC system needs to complete, using multiple input and multiple output (MIMO) based base station (BS) to sense the position and velocity of moving targets is an important aspect, which can promote the development of emerging applications such as the Internet of Vehicles and autonomous driving [5], [6], [7], [8].

The traditional moving target sensing schemes are usually implemented through frequency modulated continuous wave (FMCW) radar systems [9]. However, in communication-centric ISAC systems, researchers tend to utilize the orthogonal frequency division multiplexing (OFDM) signals to achieve the sensing function. For example, Sturm et al. proposed a distance and velocity sensing method for moving targets based on two-dimensional fast Fourier transform (2D-FFT), and provided some simulation results [10]. Multerer et al. conducted practical tests on the 2D-FFT based moving

Manuscript received 14 September 2023; accepted 11 October 2023. Date of publication 18 October 2023; date of current version 12 December 2023. This work was supported in part by Innovation and Entrepreneurship Programs for University Students at the Autonomous Region Level (S202310695107) and Intramural Programs of Tibet University for Nationalities (22MDY022). The associate editor coordinating the review of this letter and approving it for publication was F. Benkhelifa. (*Corresponding author: Meiyun Shao*.)

The authors are with the School of Information Engineering, Xizang Minzu University, Xianyang 712082, China (e-mail: xy18307109301@163.com; gao1484850962@163.com; yxr1367433018@163.com; 19169336027@163.com; myshao@xzmu.edu.cn).

Digital Object Identifier 10.1109/LCOMM.2023.3325531

targets algorithm in MIMO-OFDM system, and the test results showed that this scheme can estimate the parameters of moving targets with low accuracy [11]. Besides, Chen et al. proposed a novel code-division OFDM waveform as well as the corresponding signal processing technique, which also utilized 2D-FFT to realize target estimation [12].

Nevertheless, due to the difficulty in employing a large number of continuous subcarriers and OFDM symbols to sense the moving targets in MIMO-OFDM systems, the aforementioned 2D-FFT based moving target sensing methods are severely limited by grid resolution, which seriously affects the accuracy of sensing under relatively high signal-to-noise ratios (SNRs). In addition, the above methods only used one BS to sense the radial velocity of the target. However, with the increasing demand for sensing in intelligent scenarios, the ISAC system should consider how to obtain the actual velocity vector of the moving targets.

In this letter, we mainly focus on how to utilize massive MIMO-OFDM system to super-resolution sense the parameters of moving targets, while the communications function can easily be integrated into the communication-centric ISAC system in subsequent works. Specifically, we first propose a moving target sensing method based on estimating signal parameters via rotational variation techniques (ESPRIT) algorithm. Next, based on the results of radial velocity estimation, we propose a target actual velocity estimation scheme based on dual BSs and geometric relationships.

The remainder of this letter is organized as follows. We derive the echo channel model for MIMO-OFDM system in Section II. The moving target sensing method is proposed in Section III. The simulation results are given in Section IV, and the conclusions are given in Section V.

Notation: Lower-case and upper-case boldface letters \mathbf{a} and \mathbf{A} denote a vector and a matrix, respectively. \mathbf{a}^T and \mathbf{a}^H denote the transpose and the conjugate transpose of vector \mathbf{a} , respectively. $[\mathbf{a}]_n$ denotes the n -th element of the vector \mathbf{a} . \mathbf{e}_x and \mathbf{e}_y represent the unit vectors in the positive direction of the x-axis and y-axis. $\text{diag}(\mathbf{a})$ denotes a diagonal matrix with the diagonal elements constructed from \mathbf{a} .

II. SYSTEM MODEL

We assume that a MIMO-based BS operating in mmWave frequency band is enabled in the ISAC system. The BS is configured with a uniform linear array (ULA) composed of N antennas, and the antenna spacing is $d = \frac{\lambda}{2}$, where λ is the wavelength. Assume that the position of the n -th antenna is $(0, nd)$, where $n = 0, 1, 2, \dots, N - 1$. The BS is supposed to use the OFDM signals for sensing. Suppose that

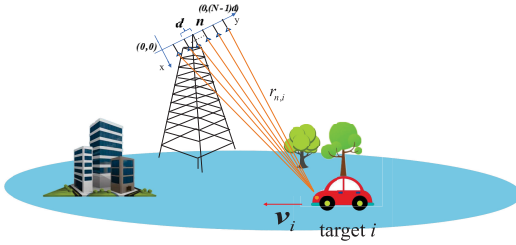


Fig. 1. System model.

there are a total of M subcarriers, whose frequencies are f_0, f_1, \dots, f_{M-1} . The subcarrier frequency interval is Δf , and $f_m = f_0 + m\Delta f$, where $m = 0, 1, \dots, M - 1$. Then the OFDM symbol duration is $T_s = \frac{1}{\Delta f}$, and the transmission bandwidth is $W = (M - 1)\Delta f$.

Assume that there are I moving targets within the sensing range of BS, in which the location of the i -th moving target is (r_i, θ_i) , and its radial velocity with respect to the BS is v_i^r . Assume that the BS uses K consecutive OFDM symbols to sense the velocity of the moving target. Then the echo channel matrix of the i -th moving target on the k -th OFDM symbol at the m -th subcarrier is

$$\mathbf{H}_{i,k,m} = \alpha_i e^{j2\pi \frac{2v_i^r}{\lambda}(k-1)T_s} e^{-j\frac{4\pi f_m r_i}{c}} \mathbf{a}(\theta_i) \mathbf{a}^T(\theta_i), \quad (1)$$

where c is the velocity of light, α_i is the fading channel factor, $\mathbf{a}(\theta_i)$ is the array steering vector, and there is

$$\mathbf{a}(\theta_i) = [1, e^{j2\pi f_0 \frac{d \sin \theta_i}{c}}, \dots, e^{j2\pi f_0 \frac{(N-1)d \sin \theta_i}{c}}]^T. \quad (2)$$

Then the total echo channel matrix of all moving targets is

$$\mathbf{H}_{k,m} = \sum_{i=1}^I \mathbf{H}_{i,k,m}. \quad (3)$$

III. MOVING TARGET SENSING METHODS

A. Moving Target Sensing Based on Single BS

MIMO arrays are typically combined with the beamforming technology to provide directional beams for the system, which is beneficial for directional sensing [13], [14]. Here we assume that the BS adopts the beamforming based on phased array structure, where each antenna is connected to a phase shifter. Then the beamforming vector towards the direction θ can be expressed as

$$\mathbf{w}(\theta) = \frac{1}{\sqrt{N}} \mathbf{a}(\theta), \quad (4)$$

which makes $|\mathbf{w}^H(\theta) \mathbf{a}(\theta)|^2 = N$. It is assumed that the sensing range required by the BS is $[\theta_{\min}, \theta_{\max}]$, all targets are within this sensing range, and the angles among the targets are different from each other. In fact, this work can easily be extended to the situations where the targets' angles are the same. We design the BS to use P times beam sweep to detect the sensing space, and the p -th beam sweep focuses on the sensing direction $\theta_p = \theta_{\min} + p \frac{\theta_{\max} - \theta_{\min}}{P-1}$, where $p = 0, 1, 2, \dots, P - 1$. Then the beamforming vector for the p -th beam sweep is $\mathbf{w}_p = \frac{1}{\sqrt{N}} \mathbf{a}(\theta_p)$. We assume that the BS transmits the known pilot signals for sensing. Then the

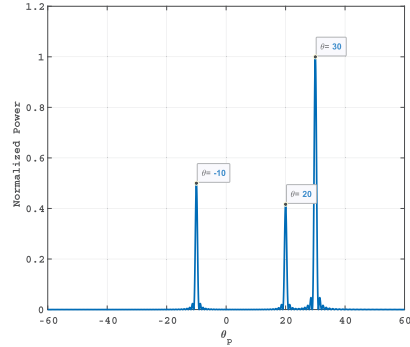


Fig. 2. An example of angle estimation, where three targets are set at $(100m, -10^\circ)$, $(120m, 20^\circ)$ and $(50m, 30^\circ)$ respectively.

echo signal on the m -th subcarrier of the k -th OFDM symbol received by the BS in the p -th beam sweep is

$$\begin{aligned} y_{p,k,m} &= \mathbf{w}_p^H \mathbf{H}_{k,m} \mathbf{w}_p^* \\ &= \frac{1}{N} \sum_{i=1}^I \alpha_i e^{j\frac{4\pi v_i^r(k-1)T_s}{\lambda}} e^{-j\frac{4\pi f_m r_i}{c}} |\mathbf{a}^H(\theta_p) \mathbf{a}(\theta_i)|^2. \end{aligned} \quad (5)$$

In massive MIMO array, when N is large enough, there is

$$|\mathbf{a}^H(\theta_p) \mathbf{a}(\theta_i)|^2 = \begin{cases} N^2 & \text{If } \theta_p = \theta_i, \\ 0 & \text{If } \theta_p \neq \theta_i. \end{cases} \quad (6)$$

We can define the total power of the echo signal in the p -th beam sweep as $G_p = \sum_{k=0}^{K-1} \sum_{m=0}^{M-1} |y_{p,k,m}|$. After P times beam sweep, the echo signal power vector can be defined as $\mathbf{G} = [G_0, G_1, \dots, G_{P-1}]^T$. Based on (5) and (6), it can be found that there will be I local peaks in \mathbf{G} , corresponding to the I targets one by one. Therefore, we perform the constant false alarm detection (CFAR) on \mathbf{G} to estimate the angle of each target, and record the beam sweep index corresponding to the i -th target as p_i . Fig. 2 shows an example of target angle estimation, where three targets are set at $(100m, -10^\circ)$, $(120m, 20^\circ)$ and $(50m, 30^\circ)$ respectively. From the figure, we can see three peaks in \mathbf{G} corresponding to three targets one by one. Hence it can estimate the angles of the three targets as -10° , 20° and 30° , respectively.

After obtaining the angle of the i -th target as $\hat{\theta}_i = \theta_{p_i}$, the echo signal corresponding to it is $y_{p_i,k,m}$, and there is

$$\begin{aligned} y_{p_i,k,m} &= \frac{1}{N} \sum_{i=1}^I \alpha_i e^{j\frac{4\pi v_i^r(k-1)T_s}{\lambda}} e^{-j\frac{4\pi f_m r_i}{c}} |\mathbf{a}^H(\theta_p) \mathbf{a}(\theta_i)|^2 \\ &\approx \alpha_{p_i} N e^{j\frac{4\pi v_{p_i}^r(k-1)T_s}{\lambda}} e^{-j\frac{4\pi f_m r_{p_i}}{c}}. \end{aligned} \quad (7)$$

Then all the $y_{p_i,k,m}$ can form a matrix $\mathbf{Y}_{p_i} \in \mathbb{C}^{K \times M}$, where $[\mathbf{Y}_{p_i}]_{k,m} = y_{p_i,k,m}$. Specifically, there is

$$\begin{aligned} \mathbf{Y}_{p_i} &= \alpha_{p_i} N \begin{bmatrix} e^{j\frac{4\pi v_{p_i}^r 0 T_s}{\lambda}} \\ \vdots \\ e^{j\frac{4\pi v_{p_i}^r (K-1) T_s}{\lambda}} \end{bmatrix} \begin{bmatrix} e^{-j\frac{4\pi f_0 r_{p_i}}{c}}, & \dots, & e^{-j\frac{4\pi f_{M-1} r_{p_i}}{c}} \end{bmatrix}. \end{aligned} \quad (8)$$

Then we can define the velocity and distance steering vectors from (9) as

$$\mathbf{a}_v(v_{pi}^r) = [1, e^{j\frac{4\pi v_{pi}}{\lambda} T_s}, \dots, e^{j\frac{4\pi v_{pi}}{\lambda} (K-1)T_s}]^T, \quad (9)$$

$$\mathbf{a}_r(r_{pi}) = [1, e^{-j\frac{4\pi r_{pi}}{c} \Delta f}, \dots, e^{-j\frac{4\pi r_{pi}}{c} (M-1)\Delta f}]^T, \quad (10)$$

respectively. And then it can be obtained that

$$\mathbf{Y}_{pi} = \alpha_{pi} N e^{-\frac{j4\pi f_0 r_{pi}}{c}} \mathbf{a}_v(v_{pi}^r) \mathbf{a}_r^T(r_{pi}). \quad (11)$$

Formula (12) means that \mathbf{Y}_{pi} can be represented as a generalized form of array signal, in which we consider $\mathbf{a}_v(v_{pi}^r)$ as a *velocity array* and all subcarriers provide multiple observations for this velocity array. Thus we can estimate the velocity of the target from \mathbf{Y}_{pi} by using a wide variety of algorithms in array signal processing. Similarly, it can be found that

$$\mathbf{Y}_{pi}^T = \alpha_{pi} N e^{-\frac{j4\pi f_0 r_{pi}}{c}} \mathbf{a}_r(r_{pi}) \mathbf{a}_v^T(v_{pi}^r). \quad (12)$$

Formula (13) means that \mathbf{Y}_{pi}^T can be considered as a generalized array signal form of the *distance array* $\mathbf{a}_r(r_{pi})$, and all OFDM symbols provide multiple observations for this distance array, which allows us to estimate target distance from \mathbf{Y}_{pi}^T .

To match the real-time and fast sensing requirements of the ISAC system, this letter considers using the ESPRIT algorithm to estimate the distance and velocity of moving targets. Firstly, the autocorrelation matrix of the observations of the velocity and distance arrays can be expressed as

$$\mathbf{R}_{pi,x,v} = \frac{1}{M} \mathbf{Y}_{pi} \mathbf{Y}_{pi}^H, \quad (13)$$

$$\mathbf{R}_{pi,x,r} = \frac{1}{K} \mathbf{Y}_{pi}^T (\mathbf{Y}_{pi}^T)^H. \quad (14)$$

Secondly, we perform eigenvalue decomposition for $\mathbf{R}_{pi,x,v}$ to obtain $\mathbf{R}_{pi,x,v} \mathbf{E}_{pi,x,v} = \Lambda_{pi,x,v} \mathbf{E}_{pi,x,v}$, where $\Lambda_{pi,x,v} = \text{diag}\{\lambda_{pi,v,1}, \lambda_{pi,v,2}, \dots, \lambda_{pi,v,K}\}$, $\lambda_{pi,v,1} \geq \lambda_{pi,v,2} \geq \dots \geq \lambda_{pi,v,K}$, and $\mathbf{E}_{pi,x,v} = [\mathbf{e}_{pi,x,v,1}, \mathbf{e}_{pi,x,v,2}, \dots, \mathbf{e}_{pi,x,v,K}]$. Thirdly, we can further estimate the number of targets in this angle direction based on the relationship between the magnitude of the eigenvalues. In this letter, it is assumed that all targets have different angles from each other. Hence only one target is included in \mathbf{Y}_{pi} . Fourthly, we take the largest eigenvalue of $\mathbf{R}_{pi,x,v}$ to form the signal subspace and divide $\mathbf{E}_{pi,x,v}$ into two parts as $\mathbf{E}_{pi,v,1}$ and $\mathbf{E}_{pi,v,2}$, and compute $\mathbf{F}_{pi,v} = \mathbf{E}_{pi,v,1}^H \mathbf{E}_{pi,v,2}$. Then the eigenvalue decomposition of $\mathbf{F}_{pi,v}$ is performed to calculate its eigenvalue $\lambda_{pi,v}$. Finally, the velocity of the i -th target can be estimated as

$$\hat{v}_i = \hat{v}_{pi} = \frac{\lambda_{pi,v} \times c}{4\pi f_0 T_s}. \quad (15)$$

Similarly, we can obtain information about the distance array as $\Lambda_{pi,x,r}$, $\mathbf{E}_{pi,x,r}$, $\mathbf{F}_{pi,r}$ and $\lambda_{pi,r}$. Then the distance of the i -th target can be estimated as

$$\hat{r}_i = \hat{r}_{pi} = -\frac{\lambda_{pi,r} \times c}{4\pi \Delta f}. \quad (16)$$

The aforementioned single BS based moving target sensing algorithm is summarized in Algorithm 1.

Algorithm 1 ESPRIT-Based Moving Target Sensing Scheme

Input: $y_{p,k,m}$ in (5) with $p = 0, 1, \dots, P-1$, $k = 0, 1, \dots, K-1$ and $m = 0, 1, \dots, M-1$.

Step 1: Calculate \mathbf{G} with $[\mathbf{G}]_p = \sum_{k=0}^{K-1} \sum_{m=0}^{M-1} |y_{p,k,m}|$, and perform CFAR on \mathbf{G} to obtain the angle estimation results for each target as $\hat{\theta}_1, \hat{\theta}_2, \dots, \hat{\theta}_I$.

Step 2: Extract the signal matrix corresponding to the i -th target from $y_{p,k,m}$ as \mathbf{Y}_{pi} .

Step 3: Calculate covariance matrices $\mathbf{R}_{pi,x,v} = \frac{1}{M} \mathbf{Y}_{pi} \mathbf{Y}_{pi}^H$ and $\mathbf{R}_{pi,x,r} = \frac{1}{K} \mathbf{Y}_{pi}^T (\mathbf{Y}_{pi}^T)^H$. Decompose them to obtain $\mathbf{E}_{pi,x,v}$ and $\mathbf{E}_{pi,x,r}$. Divide $\mathbf{E}_{pi,x,v}$ and $\mathbf{E}_{pi,x,r}$ into two parts and calculate $\mathbf{F}_{pi,v}$ and $\mathbf{F}_{pi,r}$. Then perform matrix decomposition on $\mathbf{F}_{pi,v}$ and $\mathbf{F}_{pi,r}$ to obtain $\lambda_{pi,v}$ and $\lambda_{pi,r}$.

Step 4: Calculate the distance and velocity estimates for the i -th target as $\hat{v}_i = \hat{v}_{pi} = \frac{\lambda_{pi,v} \times c}{4\pi f_0 T_s}$ and $\hat{r}_i = \hat{r}_{pi} = -\frac{\lambda_{pi,r} \times c}{4\pi \Delta f}$.

Step 5: Repeat Step 2 to Step 4 for all the I targets.

Output: $\hat{\theta}_i, \hat{v}_i$ and \hat{r}_i , where $i = 1, 2, \dots, I$.

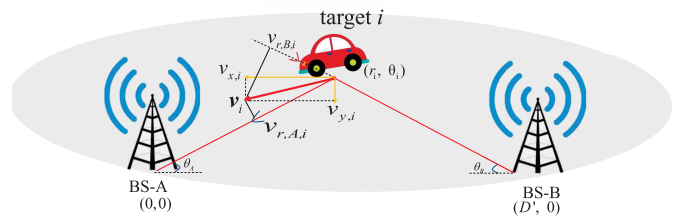


Fig. 3. System model of double BSs.

B. Actual Velocity Estimation Based on Double BSs

Using a single BS can only estimate the radial velocity of the target, while ignoring the actual velocity of the target. Here we consider adding an auxiliary BS to calculate the actual velocity of the target. As shown in Fig. 3, we name the two BSs in the system as BS-A and BS-B, respectively. Both of them are equipped with the ULA of N antennas. The centre of BS-A is located at the coordinate origin, while BS-B is parallel to BS-A, and the centre of BS-B is located at $(D', 0)$.

To begin with, the moving target sensing algorithm based on a single BS can be used to estimate the i -th target position as $(\hat{r}_i, \hat{\theta}_i)$ and the radial velocity with respect to BS-A and BS-B as $\hat{v}_{i,A}^r$ and $\hat{v}_{i,B}^r$, respectively. Assume that the actual velocity of the i -th target is $\mathbf{v}_i = v_{i,x} \mathbf{e}_x + v_{i,y} \mathbf{e}_y$. As shown in Fig. 3, according to the composition and decomposition of velocity, we can get that the relationship between the actual velocity and the radial velocity as

$$v_{i,A}^r = v_{i,x} \cos \theta_{i,A} + v_{i,y} \sin \theta_{i,A}, \quad (17)$$

$$v_{i,B}^r = v_{i,x} \cos \theta_{i,B} + v_{i,y} \sin \theta_{i,B}, \quad (18)$$

where $\theta_{i,A}$ is the angle between the line connecting the i -th target with BS-A and the positive x-axis, and $\theta_{i,B}$ is the angle between the line connecting the i -th target with BS-B and the negative x-axis. Moreover, it is known that

$$\hat{\theta}_{i,A} = \hat{\theta}_i, \quad (19)$$

$$\hat{\theta}_{i,B} = \arctan \frac{\hat{r}_i \sin \hat{\theta}_i}{D' - \hat{r}_i \cos \hat{\theta}_i}. \quad (20)$$

Then the x-axis component and y-axis component of the actual velocity of the i -th target can be estimated by combining (18), (19), (20), and (21) as

$$\hat{v}_{i,x} = \frac{\hat{v}_{i,A}^r \sin \hat{\theta}_{i,B}}{\cos \hat{\theta}_i \sin \hat{\theta}_{i,B} - \cos \hat{\theta}_{i,B} \sin \hat{\theta}_i}, \quad (21)$$

$$\hat{v}_{i,y} = \frac{\hat{v}_{i,A}^r \cos \hat{\theta}_{i,B} - \hat{v}_{i,B}^r \cos \hat{\theta}_i}{\sin \hat{\theta}_i \cos \hat{\theta}_{i,B} - \sin \hat{\theta}_{i,B} \cos \hat{\theta}_i}. \quad (22)$$

Thus we can obtain the estimation of the actual velocity as

$$\hat{\mathbf{v}}_i = \hat{v}_{i,x} \mathbf{e}_x + \hat{v}_{i,y} \mathbf{e}_y. \quad (23)$$

C. Complexity Analysis and Comparison

In this subsection, we will analyze the computational complexity of the proposed algorithm and compare it with the traditional algorithms. To begin with, we name the proposed ESPRIT-based moving target sensing algorithm as Proposed Scheme and name the traditional FFT-based sensing algorithm in [10] as Baseline Scheme.

The computational complexity of the proposed scheme mainly depends on the matrix decomposition of $\mathbf{R}_{pi,x,v}$ and $\mathbf{R}_{pi,x,r}$. Therefore, the computation complexities for distance and velocity estimation are $O(M^3)$ and $O(K^3)$, respectively. Due to the fact that the BS can estimate velocity and distance in parallel, the total computational complexity of the proposed scheme is $O(\max\{M^3, K^3\})$. The computational complexity of the baseline scheme mainly depends on the two-dimensional FFT transformation of the echo signal matrix, and its computational complexity is $O(MK \log(MK))$. Then it can be observed that the proposed scheme has a slightly higher complexity than the baseline scheme to achieve super-resolution estimation of moving targets.

IV. SIMULATION RESULTS

In the simulations, we consider the number of antennas of the BS as $N = 128$. The carrier frequency is $f_0 = 28$ GHz, and antenna spacing is $d = \frac{\lambda}{2}$. Assume that the noise is the additive complex Gaussian white noise with mean value $\mu = 0$ and variance σ^2 . We use the root mean square error (RMSE) to evaluate the sensing performance. Specifically, the RMSE for angle estimation, distance estimation, radial velocity estimation and actual velocity estimation can be defined as $\text{RMSE}_\theta = \sqrt{\frac{\sum_{q=1}^Q (\theta - \hat{\theta}_q)^2}{Q}}$, $\text{RMSE}_r = \sqrt{\frac{\sum_{q=1}^Q (r - \hat{r}_q)^2}{Q}}$, $\text{RMSE}_{v^r} = \sqrt{\frac{\sum_{q=1}^Q (v^r - \hat{v}_q^r)^2}{Q}}$, and $\text{RMSE}_v = \sqrt{\frac{\sum_{q=1}^Q ((v_x - \hat{v}_{x,q})^2 + (v_y - \hat{v}_{y,q})^2)}{Q}}$, respectively, where Q represents the number of repeated experiments, (r, θ) and $(\hat{r}_q, \hat{\theta}_q)$ are the true and estimated positions of the target, v^r and \hat{v}_q^r are the true and estimated radial velocity of the target, (v_x, v_y) and $(\hat{v}_{x,q}, \hat{v}_{y,q})$ are the true and estimated velocity vector of the target.

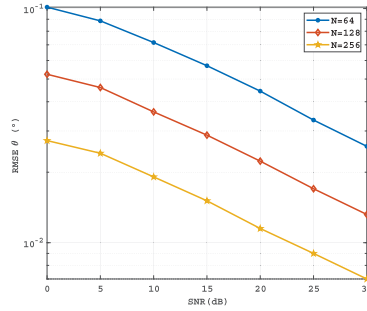


Fig. 4. The RMSE curve of angle estimation under different array sizes.

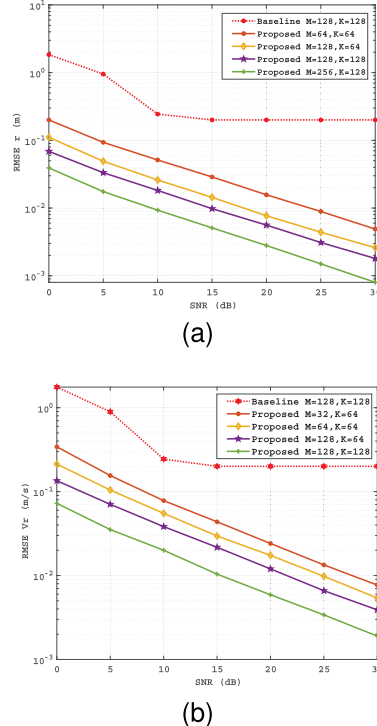


Fig. 5. (a) The RMSE curve for distance estimation of moving targets. (b) The RMSE curve for radial velocity estimation of moving targets.

A. Angle Estimation Performance

Fig. 4 shows the performance curves of target angle estimation under different antenna array sizes, where the number of subcarriers is $M = 64$, and the target is set at $(120m, 30^\circ)$. It can be seen from the figure that RMSE_θ gradually decreases with the increase of SNR. When $\text{SNR} = 0$ dB and $N = 256$, the RMSE_θ is 0.027° . When SNR increases to 20 dB, the RMSE_θ decreases to 0.011° . The simulation results demonstrate that the proposed scheme can effectively estimate the angle of the target. Moreover, it is seen that the RMSE_θ decreases with the increase of the number of antennas N , which is due to the fact that a larger antenna array can form a narrower beam, thus achieving more accurate target detection.

B. Distance and Radial Velocity Estimation Performance

We set the number of antennas as $N = 128$, and set the subcarrier frequency interval as $\Delta f = 300$ KHz. The moving target with a radial velocity of $20m/s$ is set at the position $(120m, 30^\circ)$. Fig. 5 shows the distance and radial velocity estimation performance curves under different subcarrier numbers

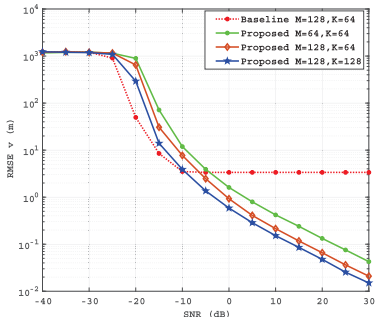


Fig. 6. The RMSE curve for actual velocity estimation.

and OFDM symbol numbers. It can be seen from the figure that the traditional FFT-based baseline method will fall into a non-zero error lower bound at high SNR, mainly because the baseline scheme is severely limited by grid resolution. Fortunately, the proposed ESPRIT-based sensing scheme can effectively achieve super-resolution estimation performance, which is more in line with the sensing requirements in emerging application scenarios.

In addition, for distance estimation, it can be seen from Fig. 5(a) that when N is fixed, RMSE_r decreases as M increases. This is mainly because a larger M can form a larger distance array, resulting in higher distance sensing accuracy. For radial velocity estimation, it can be observed from Fig. 5(b) that the RMSE_{vr} decreases with the increase of M and N . It is because larger N and M represent larger velocity array and more observations, which makes the ESPRIT algorithm more accurate in velocity estimation.

C. Actual Velocity Estimation Performance

We use double BSs to estimate the actual velocity of the target. It is assumed that BS-A and BS-B are located at $(0, 0)$ and $(90m, 0)$, respectively. The number of antennas is $N = 128$, and the subcarrier frequency interval is $\Delta f = 100$ KHz. The moving target with an actual velocity of $\mathbf{v} = (v_x, v_y) = (5m/s, 10m/s)$ is set at $(50m, 45^\circ)$. Fig. 6 shows the performance results of actual velocity sensing. It can be seen that proposed method can accurately estimate the actual velocity of the moving target. And the estimation accuracy increases with the number of subcarriers and OFDM symbols. However, by comparing the results of Fig. 6 and Fig. 5(b), it can be found that the accuracy of actual velocity estimation is slightly lower than that of radial velocity estimation under the same conditions, which is mainly due to the cumulative error in the synthesis process of the two radial velocities.

V. CONCLUSION

Integrated sensing and communications system has recently attracted lots of research interest, in which using the MIMO-OFDM system to sense the moving targets is an important

task. However, the existing FFT-based moving target estimation methods are severely limited by grid resolution, and the sensing scheme based on a single base station can only obtain the radial velocity of the target. To alleviate these issues, this letter transforms the problem of moving target sensing into a generalized array signal form, and then a moving target estimation method based on ESPRIT algorithm is proposed, realizing super-resolution and low-complexity estimation of target parameters. Moreover, we propose an actual velocity estimation scheme based on double BSs, in which the two-dimensional actual velocity vector can be estimated based on the radial velocities and the geometric relationship. Simulation results are provided to demonstrate the effectiveness of the proposed schemes.

REFERENCES

- [1] Z. Feng, Z. Fang, Z. Wei, X. Chen, Z. Quan, and D. Ji, "Joint radar and communication: A survey," *China Commun.*, vol. 17, no. 1, pp. 1–27, Jan. 2020.
- [2] X. Cheng, D. Duan, S. Gao, and L. Yang, "Integrated sensing and communications (ISAC) for vehicular communication networks (VCN)," *IEEE Internet Things J.*, vol. 9, no. 23, pp. 23441–23451, Dec. 2022.
- [3] Z. Yu, X. Hu, C. Liu, M. Peng, and C. Zhong, "Location sensing and beamforming design for IRS-enabled multi-user ISAC systems," *IEEE Trans. Signal Process.*, vol. 70, pp. 5178–5193, 2022.
- [4] Z. Xiao and Y. Zeng, "Waveform design and performance analysis for full-duplex integrated sensing and communication," *IEEE J. Sel. Areas Commun.*, vol. 40, no. 6, pp. 1823–1837, Jun. 2022.
- [5] W. Yue, C. Li, G. Mao, N. Cheng, and D. Zhou, "Evolution of road traffic congestion control: A survey from perspective of sensing, communication, and computation," *China Commun.*, vol. 18, no. 12, pp. 151–177, Dec. 2021.
- [6] P.-Y. Lai, C.-R. Dow, and Y.-Y. Chang, "Rapid-response framework for defensive driving based on Internet of Vehicles using message-oriented middleware," *IEEE Access*, vol. 6, pp. 18548–18560, 2018.
- [7] L.-L. Wang, J.-S. Gui, X.-H. Deng, F. Zeng, and Z.-F. Kuang, "Routing algorithm based on vehicle position analysis for Internet of Vehicles," *IEEE Internet Things J.*, vol. 7, no. 12, pp. 11701–11712, Dec. 2020.
- [8] X. Chen, P. Li, Q. Zhang, and Z. Jin, "Research and application of improved pure pursuit algorithm in low-speed driverless vehicle system," in *Proc. IEEE Int. Conf. Adv. Electr. Eng. Comput. Appl. (AEECA)*, Dalian, China, Aug. 2022, pp. 1483–1488.
- [9] V. Winkler, "Range Doppler detection for automotive FMCW radars," in *Proc. Eur. Radar Conf.*, Munich, Germany, Oct. 2007, pp. 166–169, doi: [10.1109/EURAD.2007.4404963](https://doi.org/10.1109/EURAD.2007.4404963).
- [10] C. Sturm and W. Wiesbeck, "Waveform design and signal processing aspects for fusion of wireless communications and radar sensing," *Proc. IEEE*, vol. 99, no. 7, pp. 1236–1259, Jul. 2011, doi: [10.1109/JPROC.2011.2131110](https://doi.org/10.1109/JPROC.2011.2131110).
- [11] T. Multerer, M. Vossiek, U. Prechtel, and V. Ziegler, "Spectrum-efficient real-time OFDM MIMO radar for moving target detection in medium-range applications," in *IEEE MTT-S Int. Microw. Symp. Dig.*, Munich, Germany, Apr. 2018, pp. 1–4, doi: [10.1109/ICMIM.2018.8443563](https://doi.org/10.1109/ICMIM.2018.8443563).
- [12] X. Chen, Z. Feng, Z. Wei, P. Zhang, and X. Yuan, "Code-division OFDM joint communication and sensing system for 6G machine-type communication," *IEEE Internet Things J.*, vol. 8, no. 15, pp. 12093–12105, Aug. 2021, doi: [10.1109/IOT.2021.3060858](https://doi.org/10.1109/IOT.2021.3060858).
- [13] L. Yan, C. Han, and Q. Ding, "Hybrid beamforming architectures of terahertz communications," in *Proc. 44th Int. Conf. Infr., Millim., THz Waves (IRMMW-THz)*, Paris, France, Sep. 2019, pp. 1–2.
- [14] C. Lin, G. Y. Li, and L. Wang, "Subarray-based coordinated beamforming training for mmWave and sub-THz communications," *IEEE J. Sel. Areas Commun.*, vol. 35, no. 9, pp. 2115–2126, Sep. 2017.